Absolute Quantification of Viral Proteins from Pseudotyped Vesicular Stomatitis Virus (VSV-GP) using Ultra High-Performance Liquid Chromatography- Multiple Reaction Monitoring (UPLC-MRM)

Rajeswari Basu[♣], Richard Dambra[*], Di Jiang[♣], Sophia A. Schätzlein[♦], Shu Njiyang[♦], Joseph Ashour[*], Abhilash I. Chiramel[♦], Adam Vigil[*], and Vladimir V. Papov, Jr[♣].

[♣] Materials and Analytical Sciences, [*] Drug Metabolism and Pharmacokinetics, Boehringer Ingelheim Pharmaceuticals, 900 Ridgebury Road, Ridgefield, Connecticut – 06877

[♦] Therapeutic Virus Development Group, Virus Therapeutic Center, Boehringer Ingelheim Pharma GmbH & Co. KG, Birkendorfer Str. 65, 88400 Biberach

(Author order was decided based on contribution)

Corresponding Authors:

* Email: rajeswari.basu@boehringer-ingelheim.com, vladimir.papov@boehringer-ingelheim.com

ABSTRACT

The rapidly developing field of oncolytic virus (OV) therapy necessitates development of new and improved analytical approaches for characterization of the virus during production and development. Accurate monitoring and absolute quantification of viral proteins is crucial for OV product characterization and can facilitate the understanding of infection, immunogenicity, and development stages of viral replication. Targeted mass spectrometry methods, like multiple reaction monitoring (MRM), offers a robust way to directly detect and quantify specific targeted proteins represented by surrogate peptides. We have leveraged the power of MRM by combining ultra-high performance liquid chromatography (UPLC) with a Sciex 6500 triple stage quadrupole mass spectrometer to develop an assay that accurately and absolutely quantifies the structural proteins of a pseudotyped vesicular stomatitis virus intended for use as a new biotherapeutic (designated hereafter as VSV-GP) to differentiate it from native VSV. The new UPLC-MRM method provides absolute quantification with the use of heavy labeled reference standard surrogate peptides. When added in known exact amounts to standards and samples, the reference standards normalize and account for any small perturbations during sample preparation and/or instrument performance, resulting in accurate and precise quantification. Because of the multiplexed nature of MRM all targeted proteins are quantified at the same time. The optimized assay has been enhanced to quantify the ratios of the processed GP1 and GP2 proteins while simultaneously measuring any remaining or unprocessed form of the envelope protein GPC (full-length GPC). (Word count 234)

IMPORTANCE

Development of oncolytic viral therapy has gained considerable momentum in the recent years. VSV-GP is a new biotherapeutic emerging in the oncolytic viral therapy platform. Novel analytical assays that can accurately and precisely quantify the viral proteins are a necessity for the successful development of viral vector as a biotherapeutic. We developed a UPLC-MRM based assay to quantify the absolute concentrations of the different structural proteins of VSV-GP. The complete processing of GPC is a pre-requisite for infectivity of the virus. The assay extends the potential for quantifying full-length GPC, which provides an understanding of the processing of GPC (along with the quantification of GP1 and GP2 separately). We used this assay in tracking GPC processing in HEK-293-F production cell lines infected with VSV-GP. (Word count-125)

INTRODUCTION

Knowledge of viral protein expression levels plays an important role in viral vector process development and therefore, a well characterized viral biotherapeutic should include an assay that can monitor the absolute concentrations of the viral proteins in purified drug product (1). The analytical methods employed toward this goal should be precise, quantitative, and reliable to ensure efficient and robust process control during production (2, 3). Proteomics-based methods can prove useful for determining protein expression levels during the virus life cycle (3, 4). While protein expression profiling is now routine in pharmaceutical research, the use of the more targeted MRM approach provides sensitive, accurate, and precise information on viral protein levels (5, 6). MRM is a tandem MS (MS/MS) scan mode that utilizes the unique capability of a triple stage quadrupole (QQQ) mass spectrometer (6–8). Target peptide molecular ions are selected by the first mass analyzer (Q1), fragmented in (Q2) by collision-induced dissociation

59 (CID) with one or several of the resultant fragment ions uniquely generated from the precursor
60 peptide ion then selected by the second mass analyzer (Q3). The precursor-fragment ion pairs
61 are termed MRM transitions that can be measured sequentially and repeatedly at a periodic
62 interval faster than the chromatographic elution of the peptide resulting in chromatographic
63 peaks for each transition which then allows simultaneous quantification of multiple peptides (9–
64 14). Quantification of full-length proteins is accomplished by generating surrogate peptides via
65 enzymatic digestion. Standard solutions are prepared using known amounts of synthetic
66 surrogate peptide and analyzed to generate standard curves for determination of the surrogate
67 peptide concentration in samples. The method can be adapted for absolute quantification by
68 spiking in known amounts of stable isotope (heavy) labeled reference standards with the exact
69 same amino acid sequence as the unlabeled surrogate peptides (15–17). The heavy standard
70 reference spikes normalize for any variability across samples (such as sample injection volume
71 or slight changes in instrument performance) making this method absolute, accurate, and precise
72 (18–20).

73 The Vesicular Stomatitis Virus (VSV) is used widely both as an oncolytic virus and vaccine
74 vector (21, 22). Herein, we use a variant of VSV that has been pseudotyped with the
75 glycoprotein (GP) from LCMV (23, 24) and apply UPLC-MRM to quantify the levels of all
76 structural proteins encoded by the VSV-GP genome. The 11 kb VSV genome encodes for 5
77 proteins: nucleocapsid (N), phosphoprotein (P), large polymerase (L), matrix (M) and surface
78 glycoprotein (GP) serving different functionalities that have been well studied (24–29) . Protein
79 composition was compared across different viral batches to assess differences in expression
80 ratios of the viral proteins and, also, to monitor for maturation of the GP complex (GPC) which
81 occurs via cleavage into the GP1 and GP2 subunits. Our results demonstrate that batch to batch

82 variability was minimal at the protein level. Furthermore, we demonstrate that, as expected, the
83 GP glycoprotein was efficiently processed over time into its individual subunits with ratios
84 indicating little or no shedding from the virus particle. This UPLC-MRM assay has proven to be
85 a powerful method for measuring viral vector proteins which in turn can provide better
86 understanding of complementary data monitoring infectivity, potency, and stability of different
87 viral batches (30, 31).

88 We then further refined the assay to include quantification of the full-length GPC before
89 processing to GP1 and GP2 subunits. We and others have observed evidence for GPC processing
90 employing semi-quantitative methods like Western Blot (**Fig. S1**) (32, 33). The GPC undergoes
91 proteolytic processing by site 1 protease (S1P) yielding two subunits, the 44-kDa peripheral GP1
92 and the 35-kDa transmembrane GP2. The prefusion form of GP1-GP2 exists as a protomer (34,
93 35) with the outer GP1 responsible for receptor engagement with its target receptor, α-
94 dystroglycan (α-DG). The receptor binding results in entry of the virus into the cells via
95 endocytosis. Subsequently, the acidic pH in the endosome triggers the dissociation of GP1 from
96 GP2 and conformational changes in GP2 drive the fusion of the virus to host membranes. By
97 independently measuring GP1 and GP2 concentrations, the GP1/GP2 ratio can provide an
98 assessment of the stoichiometry of the envelope protein complex which is known to be important
99 for infectivity (32, 36). The UPLC-MRM method developed in this study offers a new and
100 complementary approach to provide specific and quantitative insight not only into the
101 concentrations of GP1 and GP2 on the surface of the viral particles but also for any remaining
102 unprocessed GPC. Solely monitoring GP1 and GP2 levels will not identify whether the GP1 and
103 GP2 peptide surrogates are being detected from the processed or full-length unprocessed GPC.
104 Consequently, our final method contained an MRM transition for a single tryptic peptide

surrogate that is specific for the full-length unprocessed GPC in the viral samples. Using this approach, the temporal kinetics of GPC expression and processing could be evaluated in the production cells by simultaneously monitoring the changes between the three GP components (unprocessed full-length GPC, and the processed products GP1 and GP2) which provided insight into the viral lifecycle.

RESULTS

VSV-GP proteins N, P, M, GP1, GP2, and L identified by surrogate peptides

It is essential for a robust MRM assay to have the correct protein sequences and to identify suitable and specific surrogate peptides corresponding to the proteins of interest. Thus, *in-silico* sequences were first obtained from the National Center for Biotechnology Information (NCBI) database with all protein sequences from VSV except for the G-protein since the VSV used in our studies had been pseudotyped with glycoprotein from LCMV (23). To confirm these sequences were present in VSV-GP, we first carried out peptide mapping experiments using a Q-TOF mass spectrometer (Synapt G2, Waters, Milford, MA). Once the sequences were confirmed, we then proceeded to use Skyline software (University of Washington) to generate transition lists to determine potential surrogate peptides for each viral protein (37). Skyline generated virtual tryptic digests of the sequences and created a list of transitions corresponding to the individual tryptic fragments (37). The software allows the transitions and method parameters to be customized for different instrument types including our Sciex triple stage quadrupole instrument. Multiply charged precursor ions were chosen with fragment ions having *m/z* values higher than the precursor ion to improve selectivity (38). Since we intended to use C-terminally labelled internal peptide standards, y fragment ions were specifically selected for Skyline generation of

127 transitions (**Table 1**) (14, 39, 40). The sequences generated from Skyline were exported to the
128 Analyst Software for use with a Sciex 6500 triple quadrupole mass spectrometer.

129 Next, we empirically tested all the transitions to determine the optimum surrogate peptide
130 transitions using purified virus (Batch 1) that had been subjected to trypsin digestion. The
131 resultant UPLC-MRM chromatograms and a list of the most intense transitions can be found in
132 **Fig. S2** and **Supplementary XS1**, respectively. More than two transitions corresponding to a
133 particular precursor ion at the same retention time provided a first line confidence check for the
134 specificity of the transitions (41). Specificity of potential surrogate peptides for the intended viral
135 protein was then further confirmed by carrying out a NCBI Protein BLAST search to ensure
136 peptide uniqueness. Peptides confirmed to be specific to VSV-GP and having transitions
137 providing the maximum possible peak area were then selected for surrogate peptide synthesis
138 (**Table 1**).

139 We next performed the same process to identify surrogate peptides that were specific to the
140 processed GPC. Identification of a surrogate peptide for full-length GPC was more complex and
141 is discussed in the next section. Once all the optimum surrogate peptides had been identified,
142 both labeled and unlabeled forms of the surrogate peptides were synthesized for use as standards.

143

144

Table 1: Mass transitions and MRM parameters of light and heavy labeled surrogate peptides for the VSV-GP proteins in the study

Viral protein	Target peptide[a]	NCBI Ref Seq ID	Precursor ion *m/z* (Q1)	Fragment ion (Q3)	Retention Time (min)
GP1	ILFAQEK	AAF01317	424.7(+2)	622.3 (y5)	9.49
	ILFAQE**K**		428.7 (+2)	630.3 (y5)	
GP2	C[CAM]FGNTAVAK	5INE_A	484.2 (+2)	660.4 (y7)	5.71
	C[CAM]FGNNTAVA**K**		488.2 (+2)	668.4 (y7)	
P	SQWLSTIK	NP_041713.1	481.8 (+2)	747.5 (y6)	11.71
	SQWLSTI**K**		485.8 (+2)	755.5 (y6)	
L	EFLNPDER	NP_041716.1	510.2 (+2)	516.2 (y4)	9.85
	EFLNPDE**R**		515.2 (+2)	526.2 (y4)	
N	IIDNTVVPK	NP_041712.1	549.2 (+2)	871.5 (y8)	12.26
	IIDNTVVP**K**		553.3(+2)	879.5 (y8)	
M	RFNIGLYK	NP_041714.1	554.3 (+2)	310.2 (y2)	11.32
	RFNIGLKY**K**		558.3 (+2)	318.2 (y2)	

[a] The K or R residues in bold represent incorporation of heavy isotopes (^{13}C,^{15}N) resulting in a mass addition of 8 or 10 Da (K and R, respectively).

145

146

147

Table 2: Mass transitions and MRM parameters of light and heavy labeled surrogate peptides for full-length GPC

Viral protein	Target peptide[a]	NCBI Ref Seq ID	Precursor ion *m/z* (Q1)	Fragment ion (Q3)	Retention Time (min)
GPC-full Length (GPC)	LAGTFTWTLSDSSGVENPGGYC[CAM]LTK	ADO14127.1	887.8 (+3)	895.4 (y8) 1138.5(y10)	20.8
	LAGTFTWTLSDSSGVENPGGYC[CAM]LT**K**		890.5 (+3)	903.5 (y8) 1146.5 (y10)	

[a] The K residue in bold represents the incorporation of heavy (^{13}C,^{15}N) isotopes resulting in a mass addition of 8 Da.

148

149

150 **Identification and selection of surrogate peptides for GPC extends the potential of the assay**
151 **for monitoring full-length GPC**

152 The surrogate peptide for full-length GPC was selected as the sequence spanning both GP1 and
153 GP2, **Fig. S4** (33). Unlike for GP1, GP2, and the other viral peptides, the initial analysis of Batch
154 1 used for method development did not identify any detectable transitions for a full-length
155 surrogate of GPC (**Table 3**) suggesting efficient GPC processing in the purified virus sample.
156 However, we were ultimately able to detect two transitions specific for the full-length GPC
157 (from the surrogate peptide having the sequence LAGTFTWTLSDSSGVENPGGYCLTK) after
158 using a larger starting volume of purified virus which allowed us to concentrate the digest
159 approximately 10-fold using a speed-vac concentrator (**Fig. S4**). Analysis of this concentrated
160 sample by our UPLC-MRM method allowed detection of two transitions at exactly the same
161 retention time (20.8 min) which demonstrated these two transitions for this surrogate peptide
162 could be used to monitor unprocessed full-length GPC **(Table 2**). Targeted analysis of both this
163 GPC surrogate peptide and the GP1 and GP2 surrogates extends the potential of the assay,
164 enabling the assessment of GPC processing which is discussed later.

165

166 **Quantifying the major viral proteins with high precision and accuracy**

167 The relative amounts of the viral proteins in native VSV have previously been reported by other
168 groups using techniques like western-blot and transmission electron microscopy (27, 30, 42–44).
169 We used this information together with our own initial method development data to design the
170 standard concentration dilutions for each peptide standard such that all sample measurements
171 were well within the linear range (**Fig. 1**, **Table 3**). For example, the red circles in **Fig. 1** denote

172 the positions of the Batch 1 sample peptide concentrations on the linear regression line for each

173 surrogate peptide.

174 Each standard curve was derived from three technical replicates (each injected twice) with

175 calculated r^2 values ≥0.98 for all standard curves.

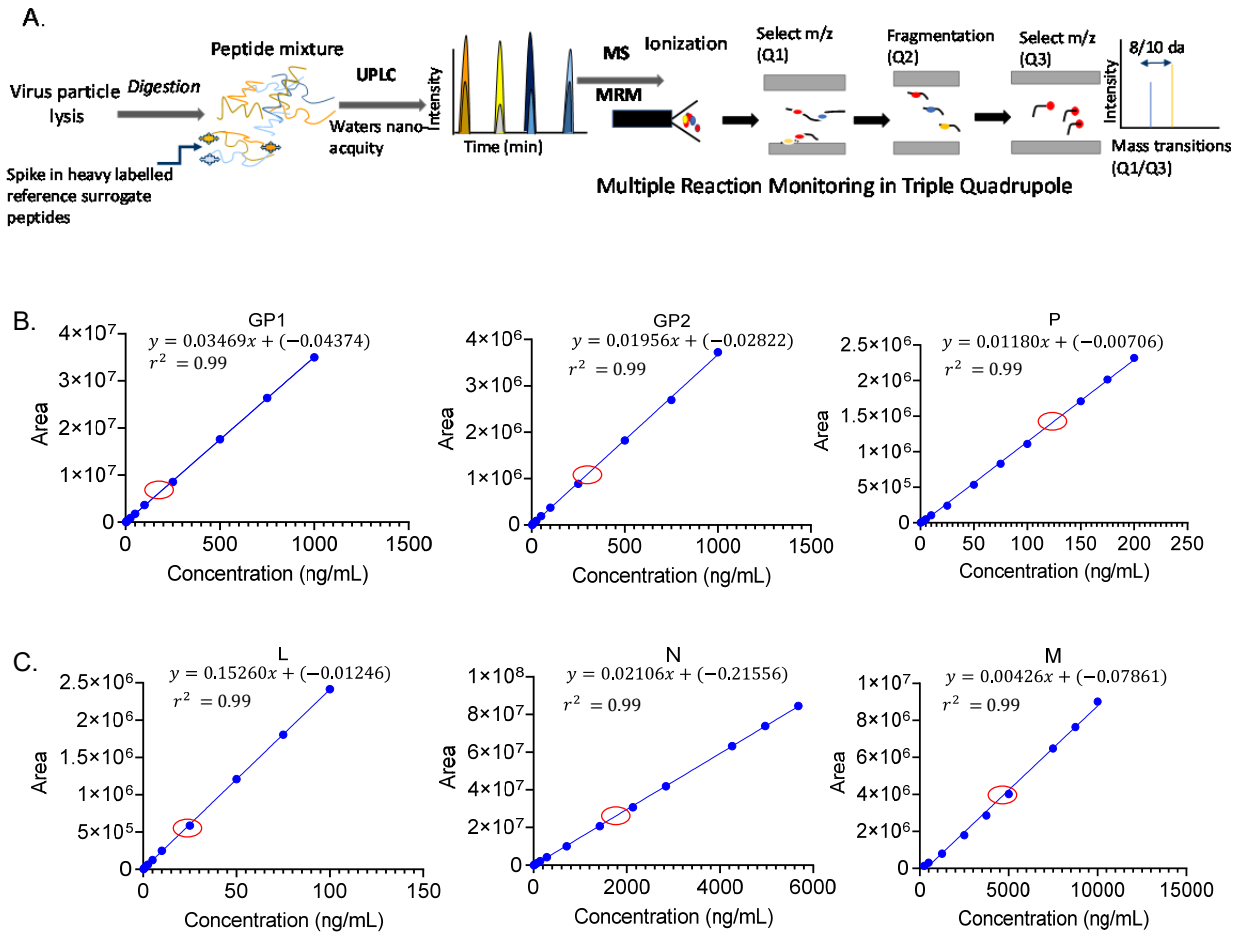

176

177

178 **Fig. 1: Schematic representation of the method and surrogate peptide standard curves A**.

179 The method used for peptide identification involves lysing the viral particles followed by

180 trypsinization using an Endo-Lys-C/trypsin protease cocktail. The resulting tryptic peptides are

181 separated using UPLC and detected via MRM on a Sciex 6500 triple stage quadrupole

182 instrument. This enables absolute quantification of the proteins corresponding to the surrogate

183 peptides. Use of MRM detection makes this method very specific and selective for the viral
184 proteins of interest. **B, C** Standard curves using unlabeled surrogate peptides for GP1, GP2, P
185 (top Panel **B**) and L, N and M (bottom panel **C**) are shown. The standard concentration ranges
186 for the peptides were adjusted empirically based on the actual concentration range of the proteins
187 present in the virus, GP1 (0.5-200 ng/mL), GP2 (0.5-200 ng/mL), P (0.5-100 ng/mL), L (0.5-100
188 ng/mL), N (7.1-5680 ng/mL) and M (25-5000 ng/mL). The red circles on the graph denote the
189 Batch 1 sample peptide concentrations. Linear regression using 1/x weighting was done with
190 MultiQuant 3.0 software which calculated the equation and r^2 values for each plot. The lowest
191 concentration of each peptide was injected 6 times to obtain the lower limit of quantification
192 (LLOQ, **Table 3**). Each linear regression (standard curve) was generated from three independent
193 runs with duplicate injections thus creating an average of six data points for each concentration.
194 The error bars represent the standard deviation of those six data points for each concentration.

195

196

197

Table 3: Concentration of surrogate peptides and corresponding VSV-GP full-length protein concentrations in Batch 1[a]

Viral Protein	Concentration of peptide (ng/mL) [b]	Monoisotopic Mass (Da)	Concentration of protein (µM) [c]	Coefficient of Variation (%) [d]	Lower limit of quantification (LLOQ)[e] (µM)
GP1	370±5	847.48	0.44±0.02	5	0.002
GP2	648±10	968.04	0.55±0.05	9	0.008
P	317±2	961.52	0.33±0.04	12	0.002
L	108±5	1018.47	0.07±0.01	12	0.001
N	1069±22	1097.65	1.42±0.2	15	0.002
M	3067±35	1106.62	2.8±0.2	14	0.012
GPC[f]	ND	2603.22	ND	ND	0.003

[a] Batch 1 was used to identify and optimize the MRM surrogate peptide transitions.
[b] The absolute concentrations of the surrogate peptides (Table 1) were calculated using MultiQuant 3.0 software. Values are the mean and standard deviation from three independent replicates (duplicate injections of each replicate).
[c] The molar protein concentrations were determined by converting surrogate peptide concentrations (ng/mL) to molar concentrations (µM).
[d] The coefficient of variation is reported for triplicates**.**
[e] LLOQ was determined by injecting the lowest concentration of each dilution series for individual peptides and using the ICH guidance LLOQ = 10 * SD/S, where SD is the standard deviation of the six injections and S is the slope of the standard curve generated for the peptide **(45).**
[f] Although GPC transitions (Table 2) were determined from Batch 1, absolute concentration measurements could not be determined (ND) due to very low GPC abundance.

198

199

200 A major strength of using mass spectrometry detection is that precursor ions from heavy

201 labeled peptides have equivalent retention time (and fragmentation pattern) to the non-labeled

202 surrogate peptide yet have a higher mass (8 or 10 Da) due to the presence of the label **(Fig. S3,**
203 **Table 2).** This feature allows unlabeled and labeled peptides with the same sequence to be
204 separated by Q1 in the mass spectrometer despite having essentially identical retention times
205 (39). In this method, the same exact amount of synthesized heavy labeled peptide is added to
206 both external standards and samples. While the amount of native (light) peptide changes
207 depending on the external standard dilution preparation the amount of heavy peptide is kept the
208 same. Since the light and heavy peptides behave identically but can be separated by a mass
209 spectrometer based on mass, this provides a very accurate and precise method for absolute
210 concentration determination that is not affected by variables such as, for example, MS signal
211 response due to slight changes in the ion source electrospray or small differences in injection
212 volume. Therefore, the x-axis in the standard curve graphs is a concentration ratio rather than
213 concentration since the peak area is normalized to the peak area of the labeled reference peptide
214 (46) as shown in **Fig. S6** with this data also demonstrating the accuracy and precision of the
215 method.

216 The development of the UPLC-MRM method for absolute quantification with an isotopically
217 labeled internal standard was based on the viral protein levels in VSV-GP Batch 1. The absolute
218 quantification of viral proteins in Batch 1 was done by spiking in the same amount of heavy
219 internal standard 50 ng/mL (for GP1, GP2, P, L and N surrogates) or 250 ng/mL (for the M
220 surrogate). As the protein M was empirically observed to be present in much higher amounts, a
221 5-fold higher concentration of M internal standard was used. Each sample was examined as a
222 technical triplicate run on the same day with three independent biological measurements
223 performed over several days. Therefore, we were able to report both intraday variability (from
224 the technical replicates) and interday variability (from the biological replicates) **(Fig. 2, Table 3)**.

225 The Coefficient of Variation (CV) for all concentration measurements was ≤15 % demonstrating
226 the excellent reproducibility of the assay **(Table 3)**. Furthermore, the relative values of each of
227 the structural proteins for VSV-GP were comparable to that reported in the literature with M and
228 N having the highest amounts and P and L having the lowest amounts (27, 30, 47). The absolute
229 concentrations of each of the proteins were calculated and expressed as molar amounts (μM)
230 **(Table 3, Fig. 2)** but were also calculated as relative concentrations [relative to M] since this is
231 the most abundant viral protein in VSV-GP **(Fig. 2, Table 5).**

232 Determination of the stability of the peptide surrogate standards is required to identify
233 appropriate storage conditions to provide accurate and reliable measurements (48). To
234 characterize in-use stability, UPLC-MRM analysis was also carried out on standard solutions
235 (dilutions) kept in storage at 4 ^{o}C for 7 days (**Fig. S5**). We observed that for all peptide curves
236 the slope changed after 7 days compared to measurements made for standard dilutions prepared
237 freshly from stock. The most extreme deviation was observed for the P protein standard peptide
238 which indicated this peptide was unstable and had undergone significant degradation within our
239 experimental time span. To determine long-term storage stability, the stock solutions were stored
240 at -25 ^{o}C and standard curve calculations were performed after one month (two freeze-thaw
241 cycles). The slope and the r^2 values were reproducible when compared to the freshly prepared
242 standards (data not shown). We therefore concluded that the stock solution of peptides could
243 tolerate storage at -25 ^{o}C for one month without undergoing degradation and could be used for
244 standard curve generation. However, we found that prolonged storage at 4 ^{o}C was not viable.

245

246

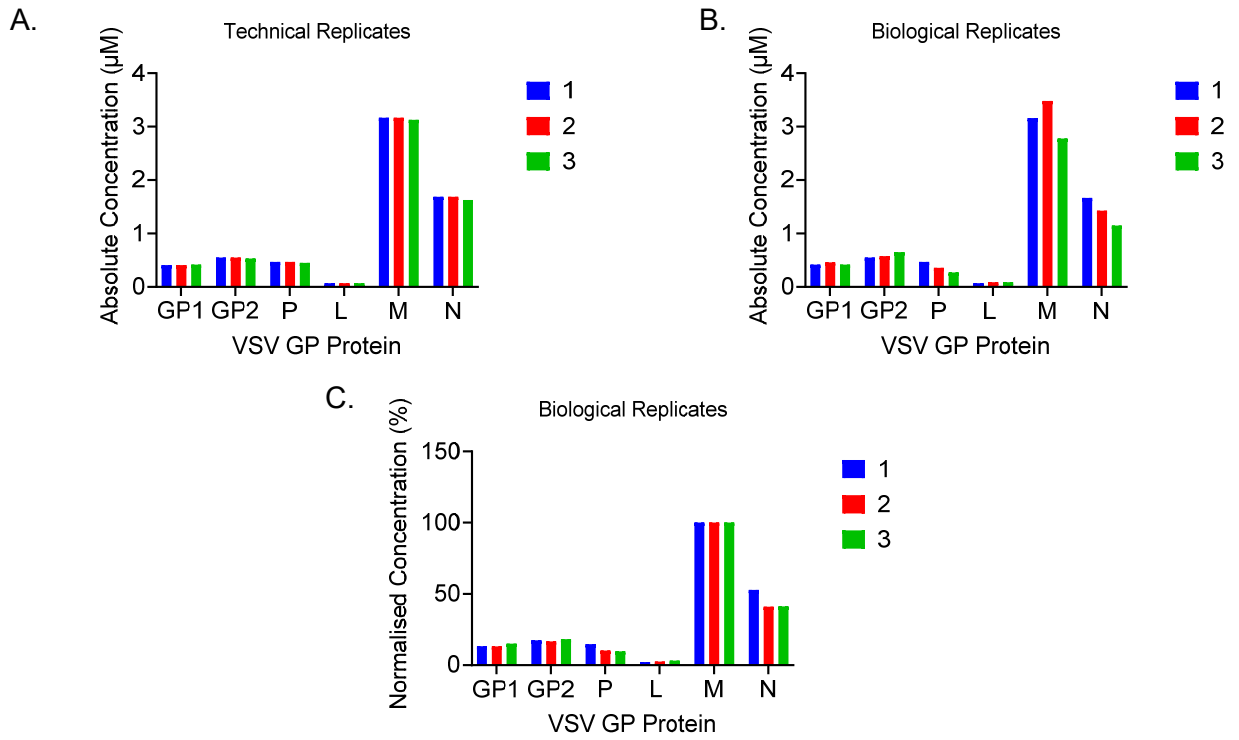

247

248 **Fig. 2**: **Concentrations of VSV-GP proteins in Batch 1**. A) Histograms of three technical
249 replicates of the same sample demonstrating intra-day variability between runs. The absolute
250 micromolar protein concentrations were calculated from the concentration of the peptide
251 reported by MultiQuant 3.0 in ng/mL and the known molecular weight of the peptides. B)
252 Histograms showing absolute concentrations of the VSV-GP proteins with three independent
253 biological samples, performed on three independent days, showing inter-day variability. Mean
254 concentrations with corresponding standard deviations are reported in **Table 3**. C). The
255 concentrations of the VSV-GP proteins normalized to the concentration of M (the most abundant
256 protein). The normalization has been done on the biological replicate samples for which absolute
257 values are plotted in (B).

258

259

260 **Comparison between different viral batches show consistency**

261 We then used our optimized method to compare viral protein abundances (and confirm GPC
262 processing) in several purified virus batches generated during process development. For this, we
263 selected 7 additional batches (Batch 2-8) and compared the protein concentrations of each batch
264 relative to Batch 1 (**Fig. 3, Table 4**). Batch 1 showed a higher absolute amount of each GP1,
265 GP2, P, L, N and M proteins with the total viral protein amounts of each batch tracking well with
266 the genome content established separately by real-time quantitative reverse transcription PCR
267 (qRT-PCR) and the infectious viral titer which was estimated by calculating average 50% Tissue
268 Culture Infectious Dose ($TCID_{50}$) (**Table S2**). For each batch it was observed that the M protein
269 was the most abundant, followed by protein N with P and L present at the lowest levels, in
270 accordance with findings by Thomas et al (42). Since the total viral protein concentrations for
271 each batch correlated with measured genome content, we also normalized the protein
272 concentrations in the same batch relative to the most abundant protein M to better understand the
273 protein concentration distributions within batches. After normalization the viral protein ratios
274 were nearly identical in each batch as indicated in **Fig. 3B, Table 5**. The GPC concentrations
275 could not be determined (as would be expected if GPC is mostly if not fully processed in the
276 purified batches) which led us to conclude the observed GP1 and GP2 concentrations were
277 measurements of GP1 and GP2 subunit proteins after GPC processing.

278

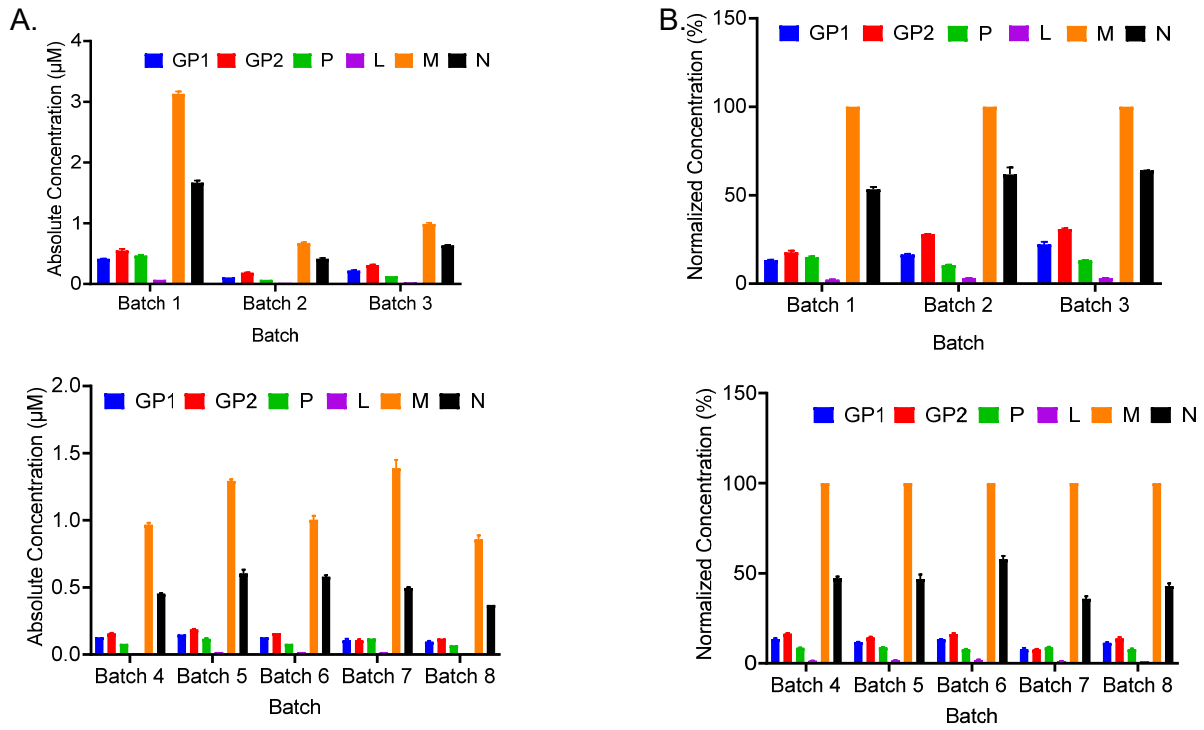

Fig. 3: Comparison of absolute and normalized concentrations of the VSV-GP proteins, between different viral batches: A) (Left Panel) Absolute concentrations (µM) of VSV-GP proteins from different developmental batches (1-8). B). (Right Panel) shows the same data but with concentrations normalized to the most abundant protein M. In all cases the plotted histograms are the mean of two samples from each batch with each sample run in triplicates, error bars representing standard deviation (**Table 4**).

288

289

Table 4: VSV-GP absolute protein concentrations for different purified viral batches

Viral Batch	Protein Concentration (µM) [a]					
	GP1	**GP2**	**P**	**L**	**N**	**M**
Batch 1[b]	0.42±0.01	0.55±0.01	0.47±0.01	0.07±0.00	1.67±0.03	3.16±0.02
Batch 2	0.21±0.01	0.24±0.01	0.09±0.01	0.03±0.01	0.47±0.02	0.95±0.01
Batch 3	0.22±0.01	0.31±0.02	0.13±0.02	0.03±0.01	0.63±0.01	0.99±0.01
Batch 4	0.13±0.01	0.15±0.02	0.08±0.01	0.01±0.00	0.45±0.02	0.98±0.01
Batch 5	0.15±0.02	0.18±0.01	0.12±0.01	0.02±0.01	0.60±0.03	1.29±0.02
Batch 6	0.13±0.01	0.16±0.01	0.08±0.01	0.02±0.01	0.58±0.01	1.00±0.01
Batch 7	0.11±0.01	0.12±0.01	0.12±0.01	0.01±0.01	0.50±0.02	1.39±0.01
Batch 8	0.11±0.01	0.12±0.01	0.07±0.01	0.01±0.00	0.37±0.01	0.89±0.01

[a] Each batch was sampled twice with each sample run in triplicate. The values reported here are average of the (6) determinations showing standard deviation. [b] Batch 1 is the batch used for development of our UPLC-MRM assay

[b] Batch 1 is the batch used for development of our UPLC-MRM assay

290

Table 5: VSV-GP protein concentrations of different purified viral batches normalized to M

Viral Batch	(%)[a]					
	GP1	**GP2**	**P**	**L**	**N**	**M**
Batch 1[b]	13.2±0.2	17.7±0.8	14.9±0.2	2.5±0.1	53.4±1.1	100
Batch 2	16.4±0.3	25.2±0.01	10.5±0.1	3.0±0.1	61.7±2.3	100
Batch 3	22.3±1.11	30.6±0.5	13.2±0.2	3.03±0.1	63.9±0.1	100
Batch 4	13.4±0.4	16.3±0.4	8.6±0.0.1	1.4±0.1	47.1±0.8	100
Batch 5	12.10±0.2	14.0±0.4	8.8±0.1	1.6±0.1	46.8±1.2	100
Batch 6	13.2±0.2	16.1±0.01	7.8±0.1	1.8±0.2	56.7±1.5	100

Batch 7	7.7±0.6	7.6±0.3	8.8±0.3	1.2±0.1	36.0±0.2	100
Batch 8	11.3±0.2	13.8±0.3	7.8±0.3	1.3±0.1	42.8±1.1	100

[a] Each batch was sampled twice with each sample run in triplicate. The values reported here are average of the (6) determinations showing standard deviation from the mean.

[b] Batch 1 is the batch used for development of our UPLC-MRM assay

291

292

293 Processing of full-length GPC into GP1 and GP2 is a prerequisite for membrane transport
294 of the virus and hence infectivity (49) (32). In addition, the outer GP2 protein associates with the
295 membrane bound GP1 but not covalently (34). For this reason, it was important to measure the
296 GP2/GP1 ratio, which can inform on both GPC processing and possible "stripping" of GP1 from
297 the viral particle surface - it has been shown earlier that during the infection process GP1 may
298 get dissociated from GP2 resulting in a slightly higher GP2 content (34, 50). Previous studies
299 have also revealed the presence of unprocessed GPC in certain viral particles with both fully and
300 partially processed GPC determined by semi-quantitative methods such as western blot assays
301 (49, 51). Building on the previous knowledge, we now have additional quantitative confidence
302 with the UPLC-MRM approach since absolute concentrations of unprocessed full-length GPC as
303 well as the post-processed subunits GP1 and GP2 can be monitored simultaneously. Our results
304 suggest that the absolute quantities of GP1 and GP2 in all the viral batches were comparable,
305 resulting in a GP2/GP1 ratio at or near 1.0 for most batches (**Table 4**). Although other studies
306 have shown that GP1 may get dissociated from GP2 during the infection process resulting in a
307 slightly higher GP2 content (50)in our VSV-GP data the ratio of GP2 to GP1 in all tested batches
308 remains very close to 1.0, suggesting not just complete processing of GPC, (32, 50, 52) but also
309 no evidence for any significant GP1 "stripping" off the surface of the viral particles.

310 The detection of MRM transitions specific to unprocessed GPC allowed us to incorporate GPC
311 specific surrogate heavy and light peptide standards into our assay. Empirically, it was observed
312 that at concentrations lower than 5 ng/mL the unlabeled GPC peptide surrogate showed poor
313 signal response which was not altogether surprising given the longer peptide length (27 amino
314 acids) (53). Consequently, higher concentrations for the GPC peptide surrogate were used
315 compared to the other VSV-GP surrogate peptides for generation of the GPC standard curve. A
316 good linear response ($r^2 \geq 0.98$) could be obtained within the concentration range of 15 ng/mL-
317 1200 ng/mL with a LLOQ of 0.003 nM providing excellent sensitivity for GPC (**Table 3, Fig.**
318 **S7**). After using a larger sample volume and concentrating via a SpeedVac, the levels of GPC
319 surrogate peptide in Batch 1 were ultimately detectable but with very low signal to noise which
320 did not allow confident calculation of GPC concentration.

321 **GPC processing can be tracked in VSV-GP infected cells over time with the UPLC-MRM**
322 **assay**

323 The quantitative measurements of the viral proteins (GP1, GP2, L, M, N, and full-length GPC)
324 discussed up until now were all obtained from purified virus batches. We next wanted to
325 examine how the protein levels might change over time. We were specifically curious to see if
326 we could capture the progress of GPC processing by exploiting the sensitivity and selectivity of
327 this assay for independently tracking GP1, GP2, and GPC. For this, we infected HEK293-F
328 (production cells) with VSV-GP at multiplicity of infection (MOI) of 0.1 and collected the cells
329 at 5 min, 3 h and 30 h time points for lysis and protein quantification by UPLC-MRM.

330 We observed a decreasing trend in GPC peak intensities in the 5 min, 3 h and 30 h time point
331 samples. The GPC peak in the 5 min sample was sufficiently abundant (within the range of the
332 standard curve) for the absolute concentration to be easily calculated (0.02±0.01 μM). However,

333 no peaks were detected for GP1 and GP2 (**Fig. 4, Table 5**). This supported the hypothesis that
334 GPC-processing to GP1 and GP2 is incomplete at the initial stage of infection. Although the 3 h
335 sample showed nearly a 2-fold lower level of GPC (0.01 μM) compared to the sample taken at 5
336 min, GP1 and GP2 remained undetectable. On the other hand, the 30 h time point sample had no
337 detectable GPC but measurable levels of GP1 and GP2 (both quantified at 0.03 μM). The
338 concentrations of GP1 and GP2 measured in these samples were significantly lower than in the
339 other viral batches we analyzed but this was expected since the latter were purified virus batches
340 (final drug product) and, hence, much more concentrated. Similarly, the remaining VSV-GP
341 proteins, while detected in the 5 min and 3h time point samples, also had lower levels compared
342 to concentrations that would be expected in the drug product. All of the viral proteins (with the
343 exception of GPC) were easily detected in the 30h time point sample. The other VSV-GP
344 proteins (P, M, N and L) also showed an increasing trend of concentration in the time -point
345 samples, with L being detectable and quantifiable in the 30 h sample. This provides further
346 support for our hypothesis that this UPLC-MRM method can track viral maturation by analysis
347 of time-point samples (**Fig. S7**). Mock cells (having no viral infection) were used as controls
348 with no surrogate peptides detected for any of the VSV-GP proteins including GPC for all time
349 points (**Table 6**). In addition, the complete viral life cycle was confirmed by $TCID_{50}$ assay,
350 which was carried out on supernatants collected at same time points (5 min, 3 h and 30 h) to
351 quantify infectious virus progeny release from cells (**Fig. S7**). In summary, we were able to
352 observe expected differences in GPC levels between the time point samples that provided
353 support for our hypothesis and demonstrated that our assay could indeed detect unprocessed
354 GPC along with a concomitant decrease in GP1 and GP2 levels.

355

356

357

Table 6: Protein concentrations for VSV-GP infected time point samples and uninfected samples [a]

Viral Batch	Protein Concentration (µM)						
	GP1	**GP2**	**GPC**	**L**	**N**	**M**	**P**
5 min	ND	ND	0.02±0.01	ND	0.02±0.01	0.02±0.00	0.01±0.02
3 h	ND	ND	0.01±0.00	ND	0.01±0.01	0.02±0.01	0.01±0.02
30 h	0.03±0.01	0.03±0.01	ND	0.01±0.0	0.19±0.02	0.34±0.02	0.07±0.03
Mock infection 5 min, 3h, 30 h	ND	ND	ND	ND	ND	ND	ND

[a] The samples were run in technical triplicates. The values reported here are average of all runs with standard deviation from the mean. ND represents Not Detected.

358

359

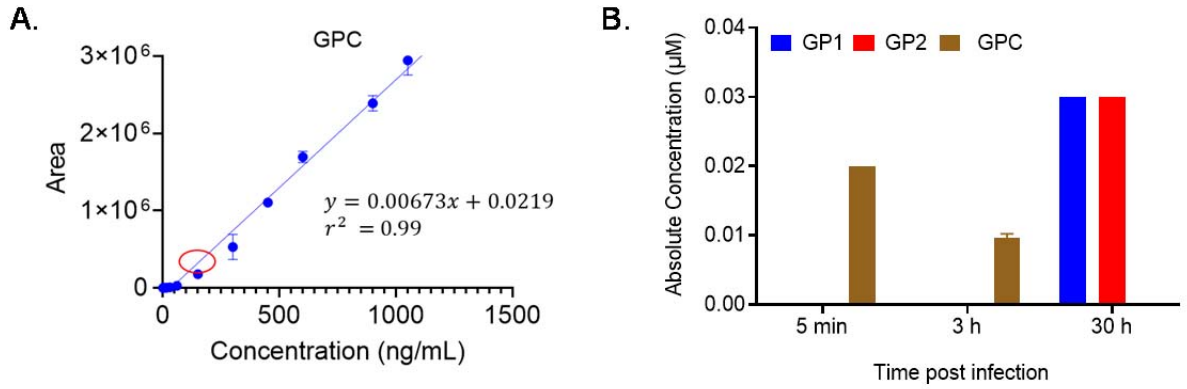

360

361

362 **Fig 4: Full-length GPC detection in time point samples of HEK-293 cells infected with**
363 **VSV-GP**: A) Standard curve with unlabeled surrogate peptide for full-length GPC (1.5-1200
364 ng/mL), the red circle showing concentration location for the earliest time point sample (5 min)
365 for which full-length GPC could be quantified. B) Concentrations of GP1, GP2 and full-length
366 GPC in time point cell pellets of HEK-293F cells infected with VSV-GP. The plotted histograms
367 are the mean of two samples from each batch with each sample run in triplicate with error bars
368 representing standard deviation. C) Time course D) Also detectable in samples after DSP

369 **DISCUSSION AND CONCLUSION**

370 The rapidly developing space of oncolytic virus therapy exemplified by VSV-GP necessitates the
371 use of novel analytical tools for characterization that are also accurate, precise, and sensitive. In
372 the present work we have harnessed the analytical power of UPLC-MRM using both isotopically
373 labeled and non-labeled surrogate peptide standards to develop an assay for absolute
374 quantification of the structural proteins encoded by VSV-GP (GP1, GP2, P, L, N and M). The
375 mature assay provided linear standard curves with nanomolar lower limits of quantification for
376 all proteins with excellent reproducibility and coefficients of variation ≤15%. The use of known
377 amounts of heavy labeled surrogate peptide added to each standard and sample increased the
378 accuracy and precision and thus, the confidence of the quantification.

379 We analyzed the absolute concentrations of the VSV-GP proteins in different purified viral
380 batches that informed us on the similarities and differences between these batches. In summary,
381 our results demonstrated a consistent trend in the protein content, with M and N being the two
382 most abundant proteins and P and L being the least abundant(42, 54–57). The differences in the
383 absolute quantity of VSV-GP proteins between the batches may reflect slight differences in the
384 production process (which is beyond the scope of this study).

385 The VSV-GP viral envelope protein is important for virus infectivity. We utilized separate
386 surrogate peptide standards for specific quantification of the two subunits GP1 and GP2 that
387 result after complete processing of the LCMV-GP protein (GPC). We also identified a third
388 tryptic peptide that could be used as a surrogate for GPC since it could only exist if GPC had not
389 been fully processed to GP1 and GP2. If unprocessed GPC was not detected (as was the case in
390 all the virus batch samples tested) we assumed that any GP1 and GP2 detected arose primarily
391 from the processed subunits. Monitoring full-length GPC together with the processed GP1 and
392 GP2 subunits also allowed us to track GPC processing. With Batch 1 used for developing the
393 assay, the GPC peptide was only detected after using a larger starting volume and concentration
394 but the signal due to GPC was still below the limit of quantification of the assay. For the other
395 batches (Batch 2-8) no GPC surrogate peptide was detected. Therefore, we concluded that in the
396 purified viral batches, the GPC processing is essentially complete with all GPC converted to GP2
397 and GP1. We further tested this hypothesis by generating samples expected to contain GPC that
398 had not been completely processed. Specifically, we infected HEK-293F cells with VSV-GP and
399 took time point samples (5 min, 3 h and 30 h) with the expectation that the earlier time points
400 would have measurable levels of unprocessed GPC. Our results show a clear distinction in the
401 levels of GPC, GP2 and GP1 detected over time, with GPC being most abundant in the 5 min
402 and to a lesser extent in the 3 h time point samples and with both 5 min and 3 h samples
403 containing no detectable GP2 and GP1. On the other hand, GP2 and GP1 were present in
404 quantifiable amounts while GPC was not detected in the 30 h time point sample. These results
405 demonstrate that the UPLC-MRM assay we developed can provide important information on
406 viral maturation as well as a snapshot of GPC processing by simultaneously measuring the levels
407 of GPC, GP1, and GP2. In addition to tracking GPC processing, the ability to analyze GP1 and

408 GP2 separately enabled us to determine the GP2/GP1 ratio which allows monitoring of any
409 potential "shedding" of the external non-membrane bound GP1 subunit of the GP2/GP1 complex
410 with higher GP2/GP1 ratios potentially an indication of GP1 dissociating from GP2 (35, 52). As
411 expected, the GP2/GP1 ratios were generally uniform in our purified virus batches with little or
412 no observed "stripping" of the outer non-membrane bound GP1.

413 In the present work, we have established the UPLC-MRM assay as a useful tool for multi-plex
414 absolute quantification of viral proteins in VSV-GP batches. The assay has the advantage of
415 being a multiplexed, selective, accurate and precise, highly sensitive, reproducible, and absolute
416 quantitative method for analysis of viral proteins for oncolytic viruses and potentially other viral
417 vectors. Although the method presented here has been used for the absolute quantification of
418 viral proteins from pseudotyped VSV-GP, it has the flexibility to be adapted for quantifying and
419 characterizing other proteins of interest such as host cell proteins and therapeutic cargo proteins.
420 Finally, our assay can be extended as a bioanalytical tool to other viral therapy platforms. (word
421 count 3336)

422 **MATERIALS AND METHODS**

423 **Chemical Reagents and Materials**

424 All experiments were carried out using Optima® LC/MS grade (Fisher Scientific, NY) water,
425 organic solvents and acids. Temperature dependent incubations for the processing of viral
426 samples and trypsinization were done using an Eppendorf Thermomixer. RapiGest for viral lysis
427 was purchased from Waters Inc, (Milford, MA). The synthesis of the surrogate peptides both
428 labeled and unlabeled was done by GenScript (Piscataway, NJ) and provided in lyophilized
429 form.

430 **Viral batch production**

431 VSV-GP virus batches were produced in HEK-293F cells in either shaker flask or bioreactor
432 formats (depending on batch ID). After infecting cells at an MOI of 0.0005, virus was purified
433 from clarified harvest via centrifugation and/or chromatographic methods similar to previous
434 reports (58, 59). The downstream processes employed were slightly unique for each batch (for
435 example the use of different purification columns or formulations).

436 **Viral protein preparation**

437 An aliquot of purified virus obtained from Development batches was concentrated in a 50 mM
438 ammonium bicarbonate solution by centrifugation at 14,800xg for 2 h. The supernatant was then
439 carefully removed, with the concentrated virus resuspended in 0.1 % RapiGest diluted in 50 mM
440 ammonium bicarbonate (pH 7.8) (60). For lysis of the virions, the suspension was sonicated for
441 15 min and then heated to 90 ^{o}C for 1 h with 300 rpm shaking before a further 15 min sonication.
442 The samples were reduced by the addition of tris (2-carboxyethyl) phosphine (TCEP) to a final
443 concentration of 20 mM and incubated at 60 ^{o}C with 600 rpm shaking for 1 h. The samples were
444 then cooled to room temperature and alkylated by the addition of iodoacetamide to a final
445 concentration of 40 mM and incubated at 37 ^{o}C with 600 rpm shaking for 30 min in the dark. A
446 mixture of trypsin and Endo-Lys-C (Trypsin/Lys-C Mix, Mass Spec Grade, Promega) was used
447 for digestion of the sample. Trypsin/LysC was reconstituted in 50 mM ammonium bicarbonate to
448 a concentration of 1 µg/ml. Samples were digested by addition of 4 µL trypsin, followed by
449 incubation at 37 ^{o}C overnight. The digestion was terminated by acidification (addition of
450 trifluoroacetic acid to a final concentration of 0.5% v/v and incubation at 37 ^{o}C for 1 h with 600
451 rpm shaking) followed by centrifugation (13,000xg for 10 min). Prepared samples not run
452 immediately by UPLC-MRM were stored at -20 ^{o}C.

453 **Calibration curve with light peptide standards**

454 The unlabeled (light) surrogate peptides corresponding to the respective viral proteins GP1, GP2,
455 P, L, N and M were synthesized by GenScript to more than 98% purity except for the surrogate
456 peptide for full-length GPC which could only be purified to 66%. All synthetic peptides were
457 supplied in a lyophilized form. Initial stock solutions were prepared to a concentration of 1
458 mg/mL by weighing and reconstituting the lyophilized peptides in LC-MS grade water having
459 0.1 % trifluoroacetic acid. A standard cocktail solution with all six peptides GP1, GP2, P, L, N
460 and M was prepared with concentrations 100, 100, 10, 10, 280 and 500 ng/µL, respectively.
461 Serial dilutions of this cocktail stock solution were then prepared to cover the expected
462 concentration range of the peptides. For GP1 and GP2 peptides, this dilution range corresponded
463 to 2.5 – 1000 ng/mL, 0.5-200 ng/mL for P, 0.5-100 ng/mL for L, 7.1- 5680 ng/mL for N and 25-
464 5000 ng/mL for M. The GPC stock solution was prepared separately at a concentration of 60
465 ng/µL. The stock solution of GPC was serially diluted to cover the concentration range 1.5-1200
466 ng/mL. The standard solutions were prepared in approximately 2-fold increments covering the
467 entire concentration range. Standards were injected from lower concentration to higher
468 concentration and each injection was done at least twice. For all analyses done in this work,
469 blank injections having only LC-MS grade water containing 0.1 % trifluoroacetic acid were used
470 liberally. For example, at least three or four blanks were run at the start of any analysis to ensure
471 system equilibration and before any standard injections. In addition, two blank injections were
472 always done after injection of the highest concentration standard to ensure there was no carry-
473 over from the previous injection. After data acquisition MultiQuant 3.0 software (Sciex, Toronto
474 Canada) was used for linear regression, calculation of r^2, and plotting of the standard curves. The

475 calibration curve thus obtained allowed for determination of concentration based on peak area
476 directly.

477 **Calibration curves with internal (heavy peptide) standards**

478 The surrogate peptides having labeled lysine ($^{13}C_6$ $^{15}N_2$) or labeled arginine ($^{13}C_6$ $^{15}N_4$) were
479 synthesized by GenScript to a purity of more than 98% and supplied in a lyophilized form. The
480 lyophilized powder of the peptides was subsequently weighed and reconstituted in LC-MS water
481 having 0.1 % trifluoroacetic acid to a final concentration of 1 mg/mL. A stock cocktail internal
482 standard solution of the labeled peptides was prepared (2 mL) containing a concentration of 2500
483 ng/mL of each surrogate peptide P, L, N, GP1, GP2 and 12500 ng/mL of surrogate peptide M
484 and GPC in LC-MS grade water having 0.1 % trifluoroacetic acid. For standard curve
485 measurements, a precise (20 µL) amount of the internal standard (labeled) heavy peptide stock
486 was added to each of the dilutions of the light standards. Each external standard solution after
487 addition of the internal standard had a final volume of 1 mL. This resulted in a final
488 concentration of the labeled P, L, N, GP1 and GP2 peptides to be 50 ng/mL whereas the final
489 concentration of the labeled M and GPC peptide was 250 ng/mL. After data acquisition
490 MultiQuant 3.0 software was used for linear regression, calculation of r^2, and plotting of the
491 standard curves. Since an internal standard was used, the calibration curve thus obtained allowed
492 for determination of concentration based on a peak area ratio.

493 **Absolute protein concentrations in viral samples with stable isotope labeled internal**
494 **standard**

495 The heavy labeled internal standard cocktail solution described above was spiked (2.45 µL) into
496 the trypsin treated viral sample (120 µL) to give a final concentration of 50 ng/mL for P, L, N,

497 GP1 and GP2 and 250 ng/mL for M surrogate peptides to match the internal standard
498 concentrations in the external standard solutions. Two samples were taken for each viral batch
499 and each sample was measured in triplicate. The calibration curve obtained from external
500 standards containing internal standards was used to determine absolute concentration of each
501 viral protein in the samples using the MultiQuant 3.0 software.

502 **Data Analysis**

503 Data analysis was performed using MultiQuant 3.0 (Sciex, Toronto, Canada). The standard
504 curves were generated using linear regression with a weighting of 1/x. A gaussian smooth width
505 of 5.0 points was applied to the peaks at the specific retention times for each of the peptides. The
506 absolute concentrations of the peptides were calculated by the software in ng/mL using a dilution
507 factor of 6. The concentration from MultiQuant in ng/mL was then converted to μM (which
508 corresponded to the full-length viral protein concentrations) using the calculated molecular
509 weight of the surrogate peptides.

510 **Determination of the Lower Limit of Quantification (LLOQ)**

511 The LLOQ determination was performed according to the ICH (International council for
512 Harmonization) standards. The lowest concentration standard was injected 6 times. LLOQ was
513 then calculated as LLOQ = 10*SD/S, where SD is the standard deviation of the six injections and
514 S is the slope of the standard curve generated for the peptide (45).

515 **Liquid Chromatography**

516 Liquid chromatography was performed on a NanoAcquity UPLC (Waters, Milford MA) with the
517 column compartment held at 60 ^{o}C and maintaining a constant flow rate of 85 μL/min through a
518 C18 reverse phased column (1 mm x 50 mm CSH, 130 Å, 1.7 μ, Waters, Milford MA). Mobile

519 phases A and B were water with 0.1 % formic acid and acetonitrile with 0.1 % formic acid,
520 respectively. In a 45 min run the peptides were separated with a linear gradient of 1-35 % B
521 within the first 35 min, followed by an increase to 90 % B within 5 mins and a re-equilibration.

522 **Time point cell-infection samples with VSV-GP**

523 The differences in GPC levels were assessed by collecting VSV-GP infected HEK293-F cells at
524 pre-determined time points. Briefly, 5 x 10^5 HEK293-F cells were plated in 12-well tissue
525 culture plates in BalanCD growth medium (1 mL). Virus stock was diluted to 5 x 10^7 $TCID_{50}$/mL
526 and infection was carried out at MOI of 1. Mock wells, without viral infection, were included as
527 controls. The cell plates were then incubated in a Kuhner LT-X shaking incubator set to 120 rpm
528 at 37 ^oC until the intended time of collection. At pre-determined time points (5 min, 3 h and 30
529 h) the contents of each well were collected into 1.5 mL collection tubes and centrifuged at 300xg
530 for 5 min to pellet the cells. The supernatant was separated without disturbing the cell pellets.
531 The cell pellets were frozen at -80 ^oC until further processing. Supernatants were collected at the
532 same time points as the cells and were analyzed by tissue culture infectious dose 50% ($TCID_{50}$)
533 assay as reported previously(58).

534 **Processing of the time point samples**

535 The frozen cell pellets were thawed at room temperature and resuspended in 0.1 % RapiGest
536 diluted in 50 mM ammonium bicarbonate (pH 7.8) containing 1 % sodium deoxycholate (61) .
537 The suspension was sonicated for 40 min and then heated to 90 ^oC for 1 h with 300 rpm shaking
538 before a further 45 min sonication. This was followed by a 10 min centrifugation at 13000 rpm to
539 pellet the cell debris. The supernatant was removed carefully into clean 1.5 mL microcentrifuge
540 tubes. The samples (supernatants) were then reduced by the addition of tris (2-carboxyethyl)

541 phosphine (TCEP) to a final concentration of 20 mM and incubated at 60 ^{o}C with 600 rpm
542 shaking for 1 h. Subsequently, they were then cooled to room temperature and alkylated by the
543 addition of iodoacetamide to a final concentration of 40 mM and incubated at 37 ^{o}C with 600
544 rpm shaking for 30 min in the dark. A mixture of trypsin and Endo-Lys-C (Trypsin/Lys-C Mix,
545 Mass Spec Grade, Promega) was used for digestion of the sample. Trypsin/LysC was
546 reconstituted in 50 mM ammonium bicarbonate to a concentration of 1 µg/ml. Samples were
547 digested by addition of 4 µL trypsin, followed by incubation at 37 ^{o}C overnight. The digestion
548 was terminated by acidification (addition of trifluoroacetic acid to a final concentration of 0.5%
549 v/v and incubation at 37 ^{o}C for 1 h with 600 rpm shaking) followed by centrifugation (13,000xg
550 for 10 min). Prepared samples not run immediately by UPLC-MRM were stored at -20 ^{o}C.

551 **Quantification of the VSV-GP protein levels in the time point samples**

552 For quantification of VSV-GP proteins in the time point samples, the cocktail of the light
553 standards was modified as follows: GP1(60 ng/µL), GP2(80 ng/ µL), GPC (60 ng/ µ L), P (10
554 ng/ µL), L (10 ng/ µL), N (280 ng/ µL) and M (500 ng/ µL). Serial dilutions of this cocktail
555 stock solution were then prepared to cover the expected concentration range of the peptides. For
556 GP1 and GPC peptides, this dilution range corresponded to 1.5– 1200 ng/mL, 2-1600 ng/mL for
557 GPC, 0.5-200 ng/mL for P, 0.5-100 ng/mL for L, 7.1- 5680 ng/mL for N and 25-5000 ng/mL for
558 M. The standard solutions were prepared in approximately 2-fold increments covering the entire
559 concentration range. A stock cocktail internal standard solution of the labeled peptides was
560 prepared (2 mL) containing a concentration of 2500 ng/mL of each surrogate peptide P, L, N,
561 GP1, GP2 and 12500 ng/mL of surrogate peptide M and GPC in LC-MS grade water having 0.1
562 % trifluoroacetic acid. For standard curve measurements, a precise (20 µL) amount of the
563 internal standard (labeled) heavy peptide stock was added to each of the dilutions of the light

564 standards and to the samples being investigated. Each external standard solution after addition
565 of the internal standard had a final volume of 1 mL. This resulted in a final concentration of the
566 labeled P, L, N, GP1 and GP2 peptides to be 50 ng/mL whereas the final concentration of the
567 labeled M and GPC peptide was 250 ng/mL.

568 **Mass Spectrometry**

569 All MRM experiments were carried out on a triple stage quadrupole mass spectrometer (6500
570 QTrap®, Sciex) using a Turbo Spray Ion Drive source in positive ion mode. Analyst Software
571 (version 7.1) was used for data acquisition with ion spray voltage set at 5200 V, curtain gas 30,
572 temperature 300 ºC, and both Gas 1 and 2 to 30 psi. Collision gas was set to 11 psi.
573 Declustering, entrance, and cell exit potentials were 80, 10, and 18 V, respectively (**Table S1**).
574 Both quadrupoles Q1 and Q3 were set to unit resolution. The dwell time for each transition was
575 adjusted to 10 ms to maintain a cycle time at or near 0.3 s to provide good delineation of the
576 UPLC peaks. Scheduled MRM was not used since all surrogate peptide peaks were well resolved
577 by the UPLC gradient method.

578 **Stability Analysis**

579 The standard stock solutions of the peptides were stored at 4 ^{o}C and run after a span of 7 days to
580 generate calibration curves as described above. The assessment of stability of the stock solutions
581 were done by analysis of the r^2 value and the slope of the curve. The peptide stock was
582 considered undergoing degradation over time if, r^2 value was less than 0.98 or the slope changed
583 when compared to freshly prepared stock solutions. Long term stability was evaluated by storage
584 of the standard stock solutions at -25 ^{o}C and analyzing the standard curves over a span of 3
585 weeks.

586 **ABBREVIATIONS**: LCMV- Lymphocytic Choriomeningitis Virus, LLOQ- Lower Limit of
587 Quantification, MRM- Multiple Reaction monitoring, qRT-PCR- Quantitative reverse
588 transcriptase polymerase chain reaction, TCID50- 50% Tissue Culture Infectious Dose, UPLC-
589 Ultra high-performance liquid chromatography, VSV- Vesicular Stomatitis Virus, VSV-GP-
590 Pseudotyped VSV with LCMV envelope protein.

591

592 **ASSOCIATED CONTENT**

593 **Supporting Information**

594 The supporting information is available .

595 Supplementary figures for chromatograms, standard curves and time point protein samples are
596 attached in word document.

597 Supplementary information for all transitions of surrogate peptides is attached in the excel sheet.

598 **AUTHOR INFORMATION**

599 **Corresponding Authors**

600 **Rajeswari Basu**- Materials and Analytical Sciences, Boehringer Ingelheim Pharmaceuticals
601 Inc., Ridgefield, Connecticut 06877; Email: rajeswari.basu@boehringer-ingelheim.com

602 **Vladimir. V. Papov**, Jr.-, Materials and Analytical Sciences, Boehringer Ingelheim
603 Pharmaceuticals Inc., Ridgefield, Connecticut 06877; Email: vladimir.papov@boehringer-
604 ingelheim.com

605 **Authors**

606 **Rajeswari Basu-** Materials and Analytical Sciences, Boehringer Ingelheim Pharmaceuticals
607 Inc., Ridgefield, Connecticut 06877; Email: rajeswari.basu@boehringer-ingelheim.com

608 **Richard Dambra** – Drug Metabolism and Pharmacokinetics, Boehringer Ingelheim
609 Pharmaceuticals Inc., Ridgefield, Connecticut 06877; Email: richard.dambra@boehringer-
610 ingelheim.com

611 **Di Jiang-** Materials and Analytical Sciences, Boehringer Ingelheim Pharmaceuticals Inc.,
612 Ridgefield, Connecticut 06877; Email: dij14002@gmail.com

613 **Sophia A. Schätzlein** - Therapeutic Virus Development Group, Virus Therapeutic Center,
614 Boehringer Ingelheim Pharma GmbH & Co. KG, 88400 Biberach; Email:
615 sophia.schaetzlein@boehringer-ingelheim.com

616 **Shu Njiyang** - Therapeutic Virus Development Group, Virus Therapeutic Center, Boehringer
617 Ingelheim Pharma GmbH & Co. KG, 88400 Biberach; Email: shu.njiyang.ext@boehringer-
618 ingelheim.com

619 **Joseph Ashour -** Drug Metabolism and Pharmacokinetics, Boehringer Ingelheim
620 Pharmaceuticals Inc., Ridgefield, Connecticut 06877; Email: joseph.ashour@boehringer-
621 ingelheim.com

622 **Abhilash I. Chiramel** - Therapeutic Virus Development Group, Virus Therapeutic Center,
623 Boehringer Ingelheim Pharma GmbH & Co. KG, 88400 Biberach; Email:
624 abhilash.chiramel@boehringer-ingelheim.com

625 **Adam Vigil-** Drug Metabolism and Pharmacokinetics, Boehringer Ingelheim Pharmaceuticals
626 Inc., Ridgefield, Connecticut 06877; Email: adam.vigil @boehringer-ingelheim.com

Vladimir. V. Papov, **Jr.-** Materials and Analytical Sciences, Boehringer Ingelheim Pharmaceuticals Inc., Ridgefield, Connecticut 06877; Email: vladimir.papov@boehringer-ingelheim.com

Present Addresses

Di Jiang: Denali Therapeutics Inc., Development Sciences, South San Francisco, CA, 94080 Email: dij14002@gmail.com

Notes

The authors declare no competing financial interests. All authors were employed by Boehringer Ingelheim Pharmaceuticals Inc. (BIPI) at the time of the experiments.

REFERENCES

1. Sanyal G, Särnefält A, Kumar A. 2021. Considerations for bioanalytical characterization and batch release of COVID-19 vaccines. Npj Vaccines 6:53.

2. González-Domínguez I, Puente-Massaguer E, Cervera L, Gòdia F. 2020. Quality Assessment of Virus-Like Particles at Single Particle Level: A Comparative Study. Viruses 12:223.

3. Lothert K, Eilts F, Wolff MW. 2022. Quantification methods for viruses and virus-like particles applied in biopharmaceutical production processes. Expert Rev Vaccines 21:1029–1044.

649 4. Lupberger J, Croonenborghs T, Suarez AAR, Renne NV, Jühling F, Oudot MA, Virzì A,
650 Bandiera S, Jamey C, Meszaros G, Brumaru D, Mukherji A, Durand SC, Heydmann L, Verrier
651 ER, Saghire HE, Hamdane N, Bartenschlager R, Fereshetian S, Ramberger E, Sinha R, Nabian
652 M, Everaert C, Jovanovic M, Mertins P, Carr SA, Chayama K, Dali-Youcef N, Ricci R,
653 Bardeesy NM, Fujiwara N, Gevaert O, Zeisel MB, Hoshida Y, Pochet N, Baumert TF. 2019.
654 Combined Analysis of Metabolomes, Proteomes, and Transcriptomes of Hepatitis C Virus–
655 Infected Cells and Liver to Identify Pathways Associated With Disease Development.
656 Gastroenterology 157:537-551.e9.

657 5. Gao Y, Fillmore TL, Munoz N, Bentley GJ, Johnson CW, Kim J, Meadows JA, Zucker JD,
658 Burnet MC, Lipton AK, Bilbao A, Orton DJ, Kim Y-M, Moore RJ, Robinson EW, Baker SE,
659 Webb-Robertson B-JM, Guss AM, Gladden JM, Beckham GT, Magnuson JK, Burnum-Johnson
660 KE. 2020. High-Throughput Large-Scale Targeted Proteomics Assays for Quantifying Pathway
661 Proteins in Pseudomonas putida KT2440. Frontiers Bioeng Biotechnology 8:603488.

662 6. Picotti P, Aebersold R. 2012. Selected reaction monitoring–based proteomics: workflows,
663 potential, pitfalls and future directions. Nat Methods 9:555–566.

664 7. Kondrat RW, Cooks RG. 1978. Direct Analysis of Mixtures by Mass Spectrometry. Analytical
665 Chemistry 50:81A-92A.

666 8. Yost RA, Enke CG. 1979. Triple quadrupole mass spectrometry for direct mixture analysis
667 and structure elucidation. Anal Chem 51:1251–1264.

668 9. Sherwood CA, Eastham A, Lee LW, Risler J, Mirzaei H, Falkner JA, Martin DB. 2009. Rapid
669 Optimization of MRM-MS Instrument Parameters by Subtle Alteration of Precursor and Product
670 m/z Targets. J Proteome Res 8:3746–3751.

671 10. Janecki DJ, Bemis KG, Tegeler TJ, Sanghani PC, Zhai L, Hurley TD, Bosron WF, Wang M.
672 2007. A multiple reaction monitoring method for absolute quantification of the human liver
673 alcohol dehydrogenase ADH1C1 isoenzyme. Anal Biochem 369:18–26.

674 11. Matraszek-Zuchowska I, Wozniak B, Posyniak A. 2016. Comparison of the Multiple
675 Reaction Monitoring and Enhanced Product Ion Scan Modes for Confirmation of Stilbenes in
676 Bovine Urine Samples Using LC–MS/MS QTRAP® System. Chromatographia 79:1003–1012.

677 12. Ulintz PJ, Yocum AK, Bodenmiller B, Aebersold R, Andrews PC, Nesvizhskii AI. 2009.
678 Comparison of MS2-Only, MSA, and MS2/MS3 Methodologies for Phosphopeptide
679 Identification. J Proteome Res 8:887–899.

680 13. A K Michael, Derek S, Juncong Y, J C Tyra, M J Angela, B H Darryl, Leigh A N, H B
681 Christoph. Multiple reaction monitoring-based, multiplexed, absolute quantitation of 45 proteins
682 in human plasma. Mol Cell Proteomics 8:1860–1877.

683 14. Peterson AC, Russell JD, Bailey DJ, Westphall MS, Coon JJ. 2012. Parallel Reaction
684 Monitoring for High Resolution and High Mass Accuracy Quantitative, Targeted Proteomics*.
685 Mol Cell Proteomics 11:1475–1488.

686 15. Kirkpatrick DS, Gerber SA, Gygi SP. 2005. The absolute quantification strategy: a general
687 procedure for the quantification of proteins and post-translational modifications. Methods
688 35:265–273.

689 16. Mayya V, Rezual K, Wu L, Fong MB, Han DK. 2006. Absolute Quantification of Multisite
690 Phosphorylation by Selective Reaction Monitoring Mass Spectrometry Determination of
691 Inhibitory Phosphorylation Status of Cyclin-Dependent Kinases* S. Mol Cell Proteomics
692 5:1146–1157.

693 17. Janecki DJ, Bemis KG, Tegeler TJ, Sanghani PC, Zhai L, Hurley TD, Bosron WF, Wang M.
694 2007. A multiple reaction monitoring method for absolute quantification of the human liver
695 alcohol dehydrogenase ADH1C1 isoenzyme. Anal Biochem 369:18–26.

696 18. Gerber SA, Kettenbach AN, Rush J, Gygi SP. 2007. Quantitative Proteomics by Mass
697 Spectrometry. Methods Mol Biology 359:71–86.

698 19. Gerber SA, Rush J, Stemman O, Kirschner MW, Gygi SP. 2003. Absolute quantification of
699 proteins and phosphoproteins from cell lysates by tandem MS. Proc National Acad Sci
700 100:6940–6945.

701 20. Salvatore S, Gerber SA, Kettenbach AN, Rush J, Gygi SP. 2006. Quantitative Proteomics by
702 Mass Spectrometry 71–86.

703 21. Riepler L, Frommelt L-S, Wilmschen-Tober S, Mbuya W, Held K, Volland A, Laer D von,
704 Geldmacher C, Kimpel J. 2023. Therapeutic Efficacy of a VSV-GP-based Human Papilloma
705 Virus Vaccine in a Murine Cancer Model. J Mol Biol 435:168096.

706 22. Tisoncik-Go J, Voss KM, Lewis TB, Muruato AE, Kuller L, Finn EE, Betancourt D,
707 Wangari S, Ahrens J, Iwayama N, Grant RF, Murnane RD, Edlefsen PT, Fuller DH, Barber GN,
708 Gale M, O'Connor MA. 2023. Evaluation of the immunogenicity and efficacy of an rVSV
709 vaccine against Zika virus infection in macaca nemestrina. Front Virol 3:1108420.

710 23. Muik A, Stubbert LJ, Jahedi RZ, Geiβ Y, Kimpel J, Dold C, Tober R, Volk A, Klein S,
711 Dietrich U, Yadollahi B, Falls T, Miletic H, Stojdl D, Bell JC, Laer D von. 2014. Re-engineering
712 Vesicular Stomatitis Virus to Abrogate Neurotoxicity, Circumvent Humoral Immunity, and
713 Enhance Oncolytic Potency. Cancer Res 74:3567–3578.

714 24. Tober R, Banki Z, Egerer L, Muik A, Behmüller S, Kreppel F, Greczmiel U, Oxenius A,
715 Laer D von, Kimpel J. 2014. VSV-GP: a Potent Viral Vaccine Vector That Boosts the Immune
716 Response upon Repeated Applications. J Virol 88:4897–4907.

717 25. Abraham G, Banerjee AK. 1976. Sequential transcription of the genes of vesicular stomatitis
718 virus. Proc National Acad Sci 73:1504–1508.

719 26. Raux H, Obiang L, Richard N, Harper F, Blondel D, Gaudin Y. 2010. The Matrix Protein of
720 Vesicular Stomatitis Virus Binds Dynamin for Efficient Viral Assembly. J Virol 84:12609–
721 12618.

722 27. Wagner RR, Schnaitman TA, Snyder RM. 1969. Structural Proteins of Vesicular Stomatitis
723 Viruses. J Virol 3:395–403.

724 28. Green TJ, Luo M. 2009. Structure of the vesicular stomatitis virus nucleocapsid in complex
725 with the nucleocapsid-binding domain of the small polymerase cofactor, P. Proc National Acad
726 Sci 106:11713–11718.

727 29. Jenni S, Bloyet L-M, Diaz-Avalos R, Liang B, Whelan SPJ, Grigorieff N, Harrison SC. 2020.
728 Structure of the Vesicular Stomatitis Virus L Protein in Complex with Its Phosphoprotein
729 Cofactor. Cell Reports 30:53-60.e5.

730 30. Wagner RR, Schnaitman TC, Snyder RM, Schnaitman CA. 1969. Protein Composition of the
731 Structural Components of Vesicular Stomatitis Virus. J Virol 3:611–618.

732 31. Bosma B, Plessis F du, Ehlert E, Nijmeijer B, Haan M de, Petry H, Lubelski J. 2018.
733 Optimization of viral protein ratios for production of rAAV serotype 5 in the baculovirus system.
734 Gene Ther 25:415–424.

735 32. Bederka LH, Bonhomme CJ, Ling EL, Buchmeier MJ. 2014. Arenavirus Stable Signal
736 Peptide Is the Keystone Subunit for Glycoprotein Complex Organization. Mbio 5:e02063-14.

737 33. Saunders AA, Ting JPC, Meisner J, Neuman BW, Perez M, Torre JC de la, Buchmeier MJ.
738 2007. Mapping the Landscape of the Lymphocytic Choriomeningitis Virus Stable Signal Peptide
739 Reveals Novel Functional Domains. J Virol 81:5649–5657.

740 34. Hastie KM, Igonet S, Sullivan BM, Legrand P, Zandonatti MA, Robinson JE, Garry RF, Rey
741 FA, Oldstone MB, Saphire EO. 2016. Crystal structure of the prefusion surface glycoprotein of
742 the prototypic arenavirus LCMV. Nat Struct Mol Biol 23:513–521.

743 35. Pennington HN, Lee J. 2022. Lassa virus glycoprotein complex review: insights into its
744 unique fusion machinery. Bioscience Rep 42:BSR20211930.

745 36. Kunz S, Edelmann KH, Torre J-C de la, Gorney R, Oldstone MBA. 2003. Mechanisms for
746 lymphocytic choriomeningitis virus glycoprotein cleavage, transport, and incorporation into
747 virions. Virology 314:168–178.

748 37. Adams KJ, Pratt B, Bose N, Dubois LG, John-Williams LS, Perrott KM, Ky K, Kapahi P,
749 Sharma V, MacCoss MJ, Moseley MA, Colton CA, MacLean BX, Schilling B, Thompson JW,

750 Consortium ADM. 2020. Skyline for Small Molecules: A Unifying Software Package for
751 Quantitative Metabolomics. J Proteome Res 19:1447–1458.

752 38. Lange V, Picotti P, Domon B, Aebersold R. 2008. Selected reaction monitoring for
753 quantitative proteomics: a tutorial. Mol Syst Biol 4:222–222.

754 39. Gerber SA, Rush J, Stemman O, Kirschner MW, Gygi SP. 2003. Absolute quantification of
755 proteins and phosphoproteins from cell lysates by tandem MS. Proc National Acad Sci
756 100:6940–6945.

757 40. Stahl-Zeng J, Lange V, Ossola R, Eckhardt K, Krek W, Aebersold R, Domon B. 2007. High
758 Sensitivity Detection of Plasma Proteins by Multiple Reaction Monitoring of N-Glycosites*. Mol
759 Cell Proteomics 6:1809–1817.

760 41. Wang C, Wang Y, Xie H, Zhan C, He X, Liu R, Hu R, Shen J, Jia Y. 2022. Establishment
761 and validation of an SIL-IS LC–MS/MS method for the determination of ibuprofen in human
762 plasma and its pharmacokinetic study. Biomed Chromatogr 36:e5287.

763 42. Thomas D, Newcomb WW, Brown JC, Wall JS, Hainfeld JF, Trus BL, Steven AC. 1985.
764 Mass and molecular composition of vesicular stomatitis virus: a scanning transmission electron
765 microscopy analysis. J Virol 54:598–607.

766 43. Barge A, Gaudin Y, Coulon P, Ruigrok RW. 1993. Vesicular stomatitis virus M protein may
767 be inside the ribonucleocapsid coil. J Virol 67:7246–7253.

768 44. Soh TK, Whelan SPJ. 2015. Tracking the Fate of Genetically Distinct Vesicular Stomatitis
769 Virus Matrix Proteins Highlights the Role for Late Domains in Assembly. J Virol 89:11750–
770 11760.

771 45. ICH guideline M10 on bioanalytical method validation and study sample analysis.

772 46. Zhang H, Liu Q, Zimmerman LJ, Ham A-JL, Slebos RJC, Rahman J, Kikuchi T, Massion
773 PP, Carbone DP, Billheimer D, Liebler DC. 2011. Methods for Peptide and Protein Quantitation
774 by Liquid Chromatography-Multiple Reaction Monitoring Mass Spectrometry*. Mol Cell
775 Proteomics 10:M110.006593.

776 47. Ball LA, Pringle CR, Flanagan B, Perepelitsa VP, Wertz GW. 1999. Phenotypic
777 Consequences of Rearranging the P, M, and G Genes of Vesicular Stomatitis Virus. J Virol
778 73:4705–4712.

779 48. Zhong X, Nayak S, Guo L, Raidas S, Zhao Y, Weiss R, Andisik M, Elango C, Sumner G,
780 Irvin SC, Partridge MA, Yan H, E SY, Qiu H, Mao Y, Torri A, Li N. 2021. Liquid
781 Chromatography-Multiple Reaction Monitoring-Mass Spectrometry Assay for Quantitative
782 Measurement of Therapeutic Antibody Cocktail REGEN-COV Concentrations in COVID-19
783 Patient Serum. Anal Chem 93:acs.analchem.1c01613.

784 49. Lenz O, Meulen J ter, Klenk H-D, Seidah NG, Garten W. 2001. The Lassa virus glycoprotein
785 precursor GP-C is proteolytically processed by subtilase SKI-1/S1P. Proc National Acad Sci
786 98:12701–12705.

787 50. Branco LM, Garry RF. 2009. Characterization of the Lassa virus GP1 ectodomain shedding:
788 implications for improved diagnostic platforms. Virol J 6:147.

789 51. Schlie K, Maisa A, Lennartz F, Ströher U, Garten W, Strecker T. 2010. Characterization of
790 Lassa Virus Glycoprotein Oligomerization and Influence of Cholesterol on Virus Replication. J
791 Virol 84:983–992.

792 52. Illick MM, Branco LM, Fair JN, Illick KA, Matschiner A, Schoepp R, Garry RF, Guttieri
793 MC. 2008. Uncoupling GP1 and GP2 expression in the Lassa virus glycoprotein complex:
794 implications for GP1 ectodomain shedding. Virol J 5:161.

795 53. Liigand P, Kaupmees K, Kruve A. 2019. Influence of the amino acid composition on the
796 ionization efficiencies of small peptides. Journal of Mass Spectrometry 54:481–487.

797 54. Redondo N, Madan V, Alvarez E, Carrasco L. 2015. Impact of Vesicular Stomatitis Virus M
798 Proteins on Different Cellular Functions. Plos One 10:e0131137.

799 55. Rosen CA, Cohen PS, Ennist HL. 1983. Identification of a new protein present in vesicular
800 stomatitis virus-infected Chinese hamster ovary cells as a degradation product of viral M protein.
801 Virology 130:331–341.

802 56. Liang B, Li Z, Jenni S, Rahmeh AA, Morin BM, Grant T, Grigorieff N, Harrison SC, Whelan
803 SPJ. 2015. Structure of the L Protein of Vesicular Stomatitis Virus from Electron
804 Cryomicroscopy. Cell 162:314–327.

805 57. Jenni S, Horwitz JA, Bloyet L-M, Whelan SPJ, Harrison SC. 2022. Visualizing molecular
806 interactions that determine assembly of a bullet-shaped vesicular stomatitis virus particle. Nat
807 Commun 13:4802.

808 58. Dambra R, Matter A, Graca K, Akhand SS, Mehta S, Bell-Cohn A, Swenson JM, Abid S,
809 Xin D, Lewis C, Coyle L, Wang M, Bunosso K, Maugiri M, Ruiz R, Cirillo CM, Fogal B,
810 Grimaldi C, Vigil A, Wood C, Ashour J. 2023. Nonclinical pharmacokinetics and biodistribution
811 of VSV-GP using methods to decouple input drug disposition and viral replication. Mol Ther -
812 Methods Clin Dev 28:190–207.

813 59. Gautam S, Xin D, Garcia AP, Spiesschaert B. 2022. Single-step rapid chromatographic
814 purification and characterization of clinical stage oncolytic VSV-GP. Frontiers Bioeng
815 Biotechnology 10:992069.

816 60. Silva JC, Gorenstein MV, Li G-Z, Vissers JPC, Geromanos SJ. 2006. Absolute
817 Quantification of Proteins by LCMSE A Virtue of Parallel ms Acquisition * S. Mol Cell
818 Proteomics 5:144–156.

819 61. Lin Y, Zhou J, Bi D, Chen P, Wang X, Liang S. 2008. Sodium-deoxycholate-assisted tryptic
820 digestion and identification of proteolytically resistant proteins. Anal Biochem 377:259–266.

821